Isomerization Dynamics of 1,1'-Diethyl-4,4'-Cyanine (1144C) Studied by Different Third-Order Nonlinear Spectroscopic Measurements

Qing-Hua Xu and Graham R. Fleming*

Department of Chemistry, University of California, Berkeley and Physical Biosciences Division, Lawrence Berkeley National Laboratory, Berkeley, California 94720

Received: May 21, 2001; In Final Form: August 6, 2001

The isomerization of 1,1'-diethyl-4,4'-cyanine (1144C) in two solvents, ethanol and hexanol, was studied by three different third-order four-wave mixing techniques: three-pulse photon echo peak shift (3PEPS), transient grating (TG), and pump−probe (PP) to provide complimentary information on different aspects of the reaction dynamics. A double-sided Feynman diagram analysis was used to assist in the formulation of the kinetic behavior in the TG and PP signals. The ground-state recovery process can be described as a single exponential process which is dominated by the bond-twisting motion on the excited-state surface. The rate is strongly viscosity and temperature dependent. A larger yield of the isomer is obtained in less viscous solvents or with greater excess excitation energy. Apparently, contradictory wavelength-dependent decay behavior was found in the TG and PP signals. This can be understood by considering the different real and imaginary contributions to the signals from hot ground-state absorption and its subsequent recovery to the equilibrated state and from the product state.

I. Introduction

The development of short laser pulses has made it possible to explore molecular motions on the time scale of femtoseconds via the nonlinear optical response.[1−3] Many different nonlinear spectroscopic techniques have been developed to probe different aspects of the molecular dynamics.[2,3] The third-order nonlinearity is the lowest order nonzero term in isotropic media and has been exploited to study the reaction dynamics in various types of four-wave mixing spectroscopies,[3−7] including photon echo, transient grating, and pump−probe measurements.

The three-pulse photon echo peak shift (3PEPS) is a novel technique that has been applied by our group and others to study solvation dynamics and energy-transfer processes for several years.[5,8−12] The insensitivity of 3PEPS to the excited-state lifetime makes it a suitable technique to study solvation dynamics and solvent effects in reactive systems.[7,13] One distinct feature of 3PEPS is its capability of differentiating the rephasing contribution and the free induction decay (FID) contribution, which contribute in a similar way to conventional population-based techniques, such as fluorescence up-conversion, pump−probe (PP), and transient grating (TG) spectroscopies.[5,10] This is the basis of the application of 3PEPS in the study of energy transfer.[10] Recently, we extended the 3PEPS technique to the study of reactive systems, such as electron transfer in electron-donating solvents[7] and torsional dynamics of the triphenylmethane (TPM) dye molecules.[14] Since 3PEPS is not sensitive to the excited-state lifetime, it can provide information on processes such as solvation and vibrational relaxation during reactions. Similar information is difficult to obtain from population-based techniques. Therefore, a combination of 3PEPS with population-based techniques such as TG or PP is attractive for the study of solution-phase reactive systems.

Photoinduced isomerization reactions have been widely studied because of their importance in nature[15−17] and as a useful model to test theories of reaction dynamics in solution.[18−25] In particular, the isomerization of 1,1'-diethyl-4,4'-cyanine (1144C) has been studied from the perspective of the solvent influence on the reaction rate.[25−29] The isomerization rates were found to be strongly dependent on the solvent viscosity, and a large amplitude bond-twisting motion was proposed to be involved in the reaction.[25−29] A model for the isomerization of 1144C is shown in Figure 1. Upon initial excitation by a short pulse, a population is created on the potential-energy surface (PES) of the first singlet excited state (S_1). Propagation of the population toward the energy minimum of S_1 surface (process 1, bond twisting) leads to a surface jump (process 2) to bring the population down to the PES of the ground state (S_0) where the energy gap between S_1 and S_0 is at a minimum. From this point, the molecule can either relax back to the original ground state or form product by moving to the PES of the ground state of the photoisomer conformation (process 3). The initial bond-twisting process was assumed to be barrierless and to occur on a subpicosecond time scale at low viscosity.[25,27,29] In addition,

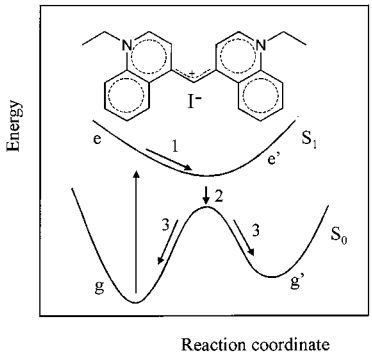

Figure 1. Schematic one-dimensional potential-energy surface for the excited-state isomerization of 1,1′-diethyl-4,4′-cyanine (1144C). A one-dimensional representation of the reaction surface is not likely to be realistic, and the sketch is intended to define the symbols in Section 3 rather than indicate the energetics of the process. The inset shows the molecular structure of 1144C.

* To whom correspondence should be addressed.

10.1021/jp011924r CCC: $20.00
Published on Web 10/20/2001

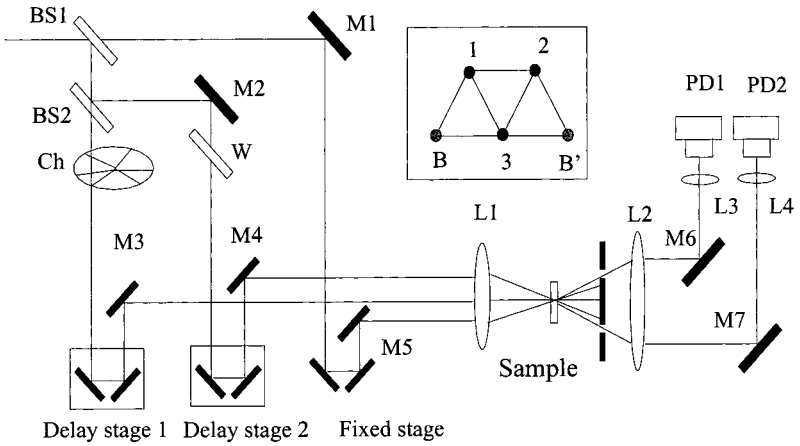

Figure 2. Experimental arrangement for 3PEPS and TG experiments and two phase matching directions $k_1 - k_2 + k_3$ (B) and $-k_1 + k_2 + k_3$ (B') in which the signals are detected. BS: beam splitter; W: compensation window; M: mirror; Ch: chopper; L: lens; PD: photodiode.

the bond-twisting process 3 on S_0 was considered to be faster than process 1 because of the steeper potential surface in S_0.[24,26,30]

In this paper, we apply the 3PEPS, TG, and PP techniques to study the isomerization of 1144C with the aim of using the different capabilities of the three techniques to provide new insights into the underlying dynamics. TG and PP are two closely related third-order four-wave mixing techniques.[3,5] The transient grating method is a homodyne technique, and the signal is the integrated square of the modulus of the third-order polarization of $P^{(3)}$, while the pump−probe signal is heterodyne detected and is proportional to the imaginary part $P^{(3)}$.[3,5,6] TG and PP measure the same dynamical information in nonreactive systems, provided the effect of acoustic gratings is negligible.[5] Myers and Hochstrasser[6] demonstrated that the interference of the accompanying acoustic grating can be ignored when the probe wavelength falls within a very strong absorption band in a simple liquid solution. In this work, in contrast to the results for nonreactive systems,[5,31] we will show that different decay behavior is observed in the TG and pump−probe measurements in the photoinduced isomerization system studied. The photon echo data provide complementary information, and the results from all three measurements can be combined to give a consistent picture of the isomerization process.

II. Experimental Section

The experimental apparatus and methods of 3PEPS and TG spectroscopy have been described in detail previously.[32] Briefly, a mode-locked Ti:sapphire oscillator (Coherent Mira) was used to seed a regenerative amplifier (Coherent RegA), the resulting 50 fs fwhm, 800 nm output was then used to pump an OPA (Coherent 9450). Nearly transform limited pulses of 40 fs fwhm at 500−700 nm with a repetition rate of 250 kHz were produced. The laser output was split into three rectilinear beams with parallel polarizations and approximately equal power. These were aligned in an equilateral triangle with each side ca. 10 mm to enable simultaneous detection of two equally phase-matched-integrated three-pulse photon echo signals. All three beams were focused by a 20 cm focal length fused silica singlet lens into the sample. A pulse energy of 5 nJ per beam before the sample was used. The experiments were also performed with energies from 3 nJ to 15 nJ, and no differences in the form of the echo signal or the peak shift were observed.

The photon echo and TG signals were detected in the phase-matching directions $-k_1 + k_2 + k_3$ and $k_1 - k_2 + k_3$ (Figure 2). For each population time T of the 3PEPS experiment, the first coherence period τ was scanned from negative to positive time delay while measuring the time-integrated echo in the two signal directions. In the TG experiment, τ was set equal to zero and T was scanned (signals from the two channels were averaged). In the PP measurement, only two beams were used, and the intensity of the probe beam was attenuated by neutral density filters to a ratio of ∼10:1 between the pump and probe beams. The signal is detected at the direction of the probe beam. The 3PEPS, TG, and PP signals were detected using Silicon photodiodes connected to lock-in amplifiers. The experiments were carried out at room temperature (290 K) unless otherwise noted.

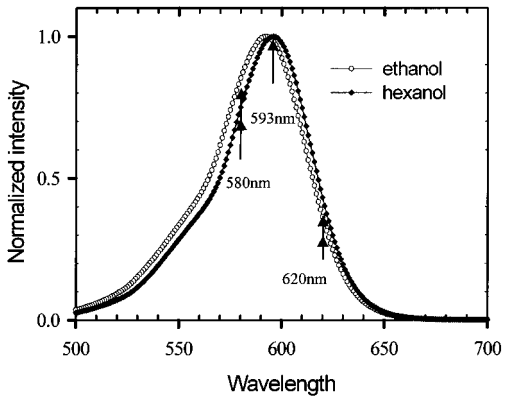

Figure 3. Absorption spectra of 1,1′-diethyl-4,4′-cyanine in ethanol and hexanol. The three wavelengths used in the experiments are indicated with the arrows.

The dye 1144C and the solvents ethanol and hexanol were purchased from Aldrich and used as received. Absorption spectra of 1144C in ethanol and hexanol shown in Figure 3 were measured using a Shimadzu UV−visible spectrophotometer. The sample was circulated through a 0.2 mm quartz flow cell, and the whole flow system was sealed to prevent evaporation of the solvent. The optical density of the sample solution was approximately 0.1 (in the 0.2 mm path length) at the absorption maximum, corresponding to a concentration of $\sim 6 \times 10^{-5}$ M, to avoid any interchromophore interaction effects.

III. Theoretical Background

All of the nonlinear spectroscopic signals can be conveniently calculated using the response function formalism.[3] The response function for the third-order signal was typically calculated with the multimode Brownian oscillator model, which has been discussed extensively by Mukamel.[3]

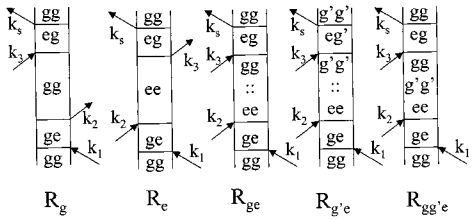

Figure 4. Double-sided Feynman diagrams for model in Figure 1. The first two terms represent the contribution from the ground- and excited-state pathways. R_{ge} represents the recovery to the relaxed ground state after photoexcitation. $R_{g'e}$ represents the contribution from the isomerized product after internal conversion. $R_{gg'e}$ represents the contribution of the decay from the isomerized product state to the original ground state. :: in R_{ge} and $R_{g'e}$ represent an evolution process from the initially excited state to the original ground state or to the isomerized ground state.

In the impulsive limit, the integrated signal in 3PEPS, TG, and PP is given by[3]

$$\text{3PEPS, TG: } S(T,\tau) = \int_0^\infty dt|P^{(3)}(t,T,\tau)|^2 \propto \int_0^\infty dt|R(t,T,\tau)|^2, \text{ for TG: } \tau=0 \quad (1a)$$

$$\text{PP: } S(T) = \mathrm{Im}\int_0^\infty dtE^*_{\mathrm{LO}}(t)P^{(3)}(t,T,0) \propto \mathrm{Re}\int_0^\infty dtE^*_{\mathrm{LO}}(t)R(t,T,0) \quad (1b)$$

where τ is the time delay between the first and second interactions (coherence time), T is the time delay between the second and third interactions (population time), and t is the time delay between the third interaction and signal field. In PP, the first and second interactions come from the same pulse (pump). $E^*_{\mathrm{LO}}(t)$ is the electric field of the probe beam, which acts as the local oscillator. In the impulsive limit, the third-order polarization $P^{(3)} \propto R$,[3] where the total response function $R = \sum R_i$, contains the molecular information about the system under study.

The most physically appealing method of modeling the nonlinear response of a system such as the one depicted in Figure 1 would be connecting a general model for the propagation of the population on the various potential surfaces and an algorithm or ansatz for the surface hopping with a calculation of the nonlinear response function. We recently described the implementation of a similar scheme for energy transfer in weakly coupled disordered molecular aggregates in which a Monte Carlo/Master equation description of the population dynamics was interfaced with the response function calculation.[33,34] However, for the continually evolving population dynamics appropriate to an isomerizing molecule, such a formalism remains to be constructed and for the present analysis we use a considerably simpler approach based on assigning response functions to different regions of the potential-energy surface which are then connected via a simple kinetic scheme.

In the isomerization reaction shown in Figure 1, if the product yield (branching ratio) is α, our strategy is to break up the total response function into five terms corresponding to the different regions of the potential surfaces which give rise to signals at various times in the overall process. Double-sided Feynman diagrams for each term are shown in Figure 4.

$$R = R_g + R_e - (1-\alpha)R_{ge} - \alpha R_{g'e} - \alpha R_{gg'e} \quad (2)$$

Here we also include the back-reaction process from the isomerized product to the original ground state (this process is not shown in Figure 1). The first two terms correspond to the contribution from the hole on the ground state (R_g) and the population on the excited state (R_e). R_{ge} corresponds to the contribution from the recovery of the excited-state population to the original ground state. $R_{g'e}$, corresponding to the contribution from the isomerized product state, also needs to be included when the absorption of the reactant and isomerized product ground state overlap spectrally. $R_{gg'e}$ corresponds to the contribution from the recovery of the isomerized product state back to the original ground state. The negative sign of the last three terms arises from the odd number of interactions with the ket and bra sides of the double-sided Feynman diagrams.[3]

Since reaction does not occur in the ground state, R_g is not affected by the reaction and contains only the contribution from solvation dynamics. $R_g = R^0_g$. Hereafter, the superscript 0 denotes that a separation between solvation dynamics and population kinetics has been made. However, R_e needs to be properly scaled according to the corresponding population kinetics on the excited state. For simplicity, we will assume Markovian population kinetics. In this case, we can write $R_e = R^0_e e^{-T/\tau_a}$, where τ_a is the time scale on which the molecules in the excited state move out the probe laser window.

The ground-state recovery process is described by R_{ge}. If only one process with rate τ_b dominates the whole process, then $R_{ge} = R^0_{ge}(1 - e^{-T/\tau_b})$. The effect of solvation dynamics in the excited state is to bring the molecules back to the ground state at a different position of the solvation coordinate. We refer to this in ref 13 as the history effect. If this effect is ignored, $R^0_{ge} = R^0_g$. Thus $R_g - R_{ge} = R^0_g e^{-T/\tau_b}$.[13]

When all the excited-state population recovers back to the original ground state or the branching ratio is low ($\alpha \sim 0$), only the first three terms need to be considered. In this case, the whole response function can be simplified to

$$R = R^0_e e^{-T/\tau_a} + R^0_g e^{-T/\tau_b} \quad (3)$$

In case of a large branching ratio, if the photoisomer absorption is also resonant with the laser wavelength, an additional term, $-R_{g'e}$, is required. $R_{g'e} = R^0_{g'e}(e^{-T/\tau_d} - e^{-T/\tau_c})$, where τ_c is the rate-determining step from the excited state to the isomerized ground state, and τ_d is the rate of the back-reaction from the isomerized product to the original ground state. The condition $\tau_c \ll \tau_d$ is assumed here.

Similarly, the contribution from the return of the isomerized product state to the original ground state, $R_{gg'e}$, can be approximated as $R_{gg'e} = R^0_{gg'e}(1 - e^{-T/\tau_d})$ when $\tau_c \ll \tau_d$.

The total response function is given by

$$\begin{aligned} R &= R_g + R_e - (1-\alpha)R_{ge} - \alpha R_{g'e} - \alpha R_{gg'e} \\ &= R^0_g + R^0_e e^{-T/\tau_a} - (1-\alpha)R^0_{ge}(1 - e^{-T/\tau_b}) - \alpha R^0_{g'e}(e^{-T/\tau_d} - e^{-T/\tau_c}) - \alpha R^0_{gg'e}(1 - e^{-T/\tau_a}) \\ &= R^0_e e^{-T/\tau_a} + (1-\alpha)R^0_{ge}e^{-T/\tau_b} + \alpha R^0_{g'e}e^{-T/\tau_c} + \alpha(R^0_{gg'e} - R^0_{g'e})e^{-T/\tau_d} + [R^0_{gg} - (1-\alpha)R^0_{ge} - \alpha R^0_{ge'e}] \\ &= R^0_e e^{-T/\tau_a} + (1-\alpha)R^0_g e^{-T/\tau_b} + \alpha R^0_{g'e}e^{-T/\tau_c} + \alpha(R^0_{gg'e} - R^0_{g'e})e^{-T/\tau_d} \end{aligned} \quad (4)$$

In the above formula, $R^0_{gg'e} = R^0_{ge} = R^0_g$ is assumed by ignoring the history effect.[13] When the back-reaction from the product to the original ground state is very slow (τ_d is very large), the last term $R_{gg'e}$ will not contribute. The above formula

is then simplified to

$$R = R^0_e e^{-T/\tau_a} + (1-\alpha)R^0_{ge} e^{-T/\tau_b} + \alpha R^0_{g'e} e^{-T/\tau_c} + \alpha[R^0_g - R^0_{g'e}] \quad (5)$$

When the absorption coefficients at the measuring wavelength and the recovery time scales are similar ($\tau_b \sim \tau_c$) for both ground-state isomers, as in the current system 1144C, which is discussed in detail in section V. A., the TG and PP techniques cannot distinguish between the two contributions. But the two contributions can appear differently in 3PEPS, which has the capability of differentiating the rephasing and FID contributions. Even when τ_b and τ_c differ, in some systems with very different decay paths for the two different ground-state recovery processes, nonexponential decay behavior will be obtained in the pump−probe and transient grating techniques. However, similar nonexponential decay profiles can also arise from the decay to one ground state if the time scales of the different steps during the recovery processes are comparable. This subtle difference can be revealed in a 3PEPS measurement.

For simplicity, a contribution from the hot ground state was not included in the above formulas. This contribution can be treated as a transient product state during the recovery process and can be easily included in a similar way.[35]

In the context of the above formulas, the signal is defined in terms of transmission intensity rather than the conventional transient absorption in the pump−probe experiment, thus the stimulated emission (R_e) and ground-state bleaching (R_g) contribute as positive terms, while excited-state absorption, hot ground-state absorption, and product state absorption ($-R_{g'e}$) contribute as negative terms. This convention allows the pump−probe and transient grating signals to be discussed in a consistent manner.

IV. Results

IV. A. Wavelength-Dependent Transient Grating (TG) Measurements. TG measurements for 1144C in ethanol and hexanol were performed at three different wavelengths: 580, 593, and 620 nm (Figure 5), which are located on the blue side, the peak position, and the red edge of the absorption band, respectively (Figure 3). Since these three wavelengths are strongly resonant with the S_0–S_1 electronic transition, the TG signal will be dominated by the electronic contribution, and the contribution of the acoustic grating can be ignored (even in the existence of acoustic grating, its oscillation period is several nanoseconds and its rise time is much longer than the time scale here).[6] Since the homodyne TG signal is the integrated square of the modulus of the third-order polarization, the square root of the signals was fit using a sum of exponential components. At 580 and 593 nm, the square root of the TG signal can be well fit with a biexponential decay consisting of a fast component of ~100 fs and a slow component with a lifetime of several picoseconds. At 620 nm, an additional component with a small negative amplitude is needed to give a better fit. The results of the biexponential fitting are summarized in Table 1.

Since TG probes the dynamics both on the excited-state and ground-state pathways,[5,14] the biexponential decay can be directly related to the relaxation processes in these states (eq 3). We ascribe the shorter decay time to the stimulated emission (SE) lifetime, corresponding to the initial prepared wave packet moving out of the Franck−Condon region on S_1. The longer decay time is ascribed to the time scale of ground-state recovery (GSR). GSR monitors the total relaxation process from the initially prepared excited-state conformation back to the original ground-state conformation, including the relaxation on both the excited- and ground-state surfaces. In general, the GSR will be nonexponential unless one of the rates associated with decay on the excited-state surface (process 1), internal conversion (process 2), and ground-state surface (process 3) is much slower than the others.

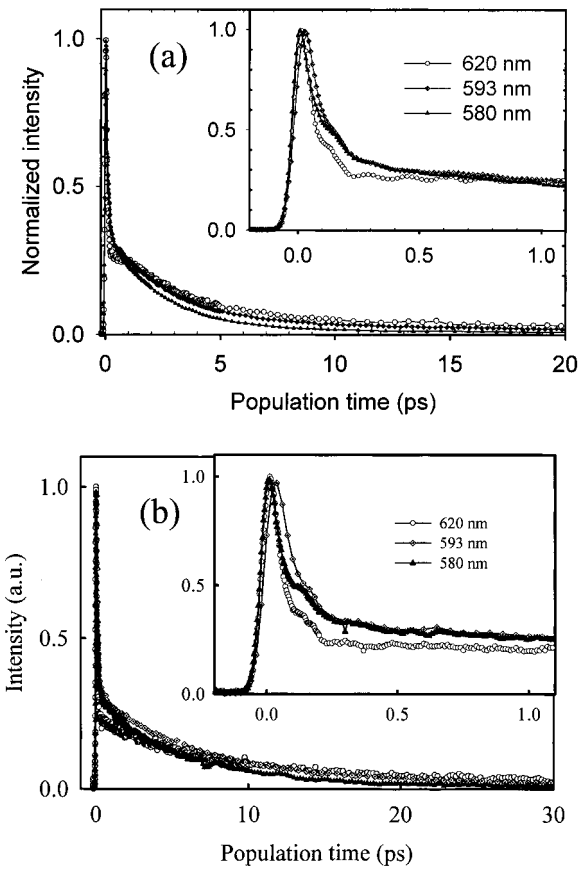

Figure 5. Transient grating measurements for 1144C in ethanol (a) and hexanol (b) at three different excitation wavelengths: 580, 593, and 620 nm.

TABLE 1: Transient Grating Data for 1144C in Ethanol and Hexanol at Different Wavelengths[a]

solvent	wavelength	A_1	τ_1 (fs)	A_2	τ_2 (ps)
ethanol	620 nm	0.64	56	0.36	5.2
	593 nm	0.58	86	0.42	4.4
	580 nm	0.46	100	0.54	3.9
hexanol	620 nm	0.64	80	0.36	11.7
	593 nm	0.58	104	0.42	11.8
	580 nm	0.46	125	0.54	9.1

[a] The data are fit with two exponentials after taking the square root of the signal. The small negative component for 620 nm data is not listed in the table.

From Table 1 and Figure 5, we can see that both the SE and GSR lifetimes in ethanol are smaller than those in hexanol at all three wavelengths. The strong viscosity dependence of the GSR lifetimes has been attributed to a large amplitude bond-twisting motion involved in the reactions.[23] However, different wavelength dependencies of the SE and GSR lifetimes were observed. The SE rate decreases with a blue shift of the excitation wavelength, while the corresponding GSR rates increases slightly.

TG measurements for 1144C in ethanol and hexanol were also carried out at three different temperatures: 10, 40, and 70

TABLE 2: Temperature-Dependent TG Results for 1144C in Ethanol and Hexanol (580 nm)[a]

solvent	T	viscosity (cP)	A_1	τ_1 (fs)	A_2	τ_2 (ps)
ethanol	10 °C	1.466	0.51	105	0.49	4.0
	40 °C	0.834	0.47	102	0.53	3.6
	70 °C	0.504	0.51	98	0.49	3.0
hexanol	10 °C	7.468	0.49	144	0.51	10.1
	40 °C	2.996	0.50	132	0.50	8.0
	70 °C	1.410	0.48	120	0.52	5.7

[a] Data were fitted to a sum of two exponentials after taking the square root of the signal.

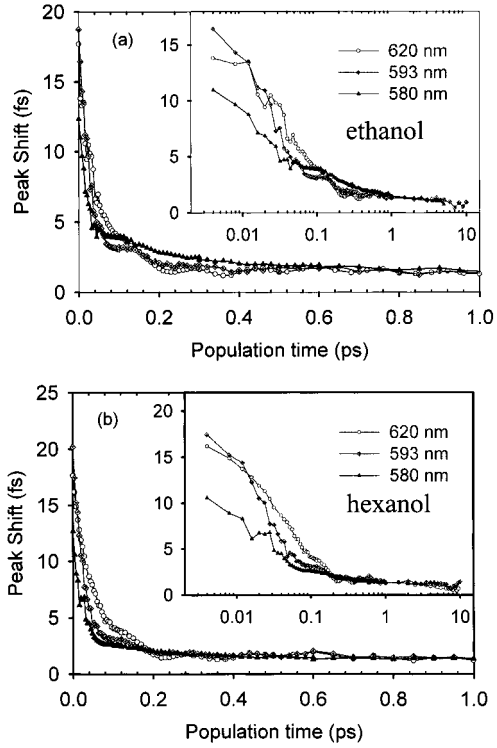

Figure 6. 3PEPS measurements for 1144C in ethanol (a) and hexanol (b) at three different excitation wavelengths: 580, 593, and 620 nm.

°C. The excitation wavelength was fixed at 580 nm since simple biexponential decay was obtained at this wavelength. The results of biexponential fits to the square root of the TG signals are listed in Table 2. The short SE lifetime is only weakly sensitive to the temperature, with a slight shortening at higher temperatures. In contrast, as would be expected from the decrease of viscosity with temperature, the GSR lifetime is strongly dependent on the temperature, becoming significantly shorter at higher temperatures.

IV. B. Wavelength-Dependent 3PEPS Measurements. 3PEPS measurements for 1144C in ethanol and hexanol were carried out at the same wavelengths as in the TG experiments (Figure 6). When the excitation wavelength is shifted to a shorter wavelength, the peak shift decays faster at short times and then becomes flatter at later times. A similar wavelength-dependent peak shift decay was also observed in many nonreactive and reactive systems.[14,36,37] However, the peak shift in ethanol at 580 nm shows a strikingly different effect. In the time range from 100 to 500 fs, the peak shift is significantly larger than what is observed at 593 and 620 nm.

To facilitate comparison, the 3PEPS data for the two solvents at each wavelength are plotted on the same graph in Figure 7. At 593 and 620 nm, the 3PEPS curves of 1144C in ethanol and hexanol are very similar and only subtle differences were

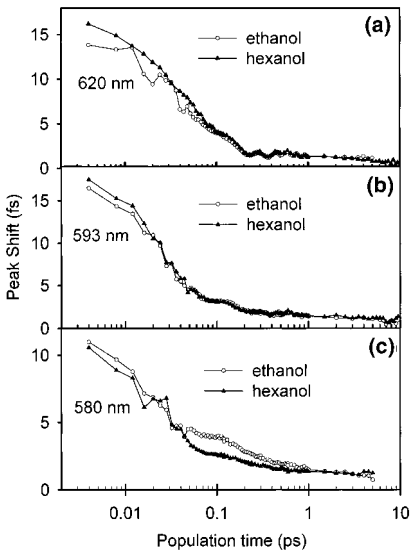

Figure 7. 3PEPS data for 1144C in ethanol and hexanol at the same excitation wavelength are shown on the same plot: (a) 620 nm; (b) 593 nm; (c) 580 nm.

observed, arising from the different solvation time scales of the two solvents.[5] The similarity of the 3PEPS data in the two solvents, which have different viscosities and very different reaction rates, on the other hand, confirms that 3PEPS is not sensitive to the excited-state lifetime.[5] In contrast, remarkably different peak shifts were observed in the two solvents at 580 nm. The peak shift in ethanol is larger than that in hexanol from 50 fs to 2 ps. Such a solvent dependence in the 3PEPS signal at 580 nm cannot be simply explained by the standard two- or three-level system models.[13,38]

Of course, the isomerization of 1144C is not a simple two- or three-level system. In 1144C, two forms of the ground-state exist, and the excited-state population decays to both forms.[27−29] The absorption spectrum of the isomerization product has been found to be only slightly red shifted with respect to the original ground state.[28,29] This leads us to suggest that the abnormal peak shift behavior in ethanol at 580 nm could be due to a contribution from the product-state contribution. If the absorption coefficients at this wavelength of the reactant ground state and the product ground-state absorption are different, a finite constant value in the response function will result after isomerization due to the different values of R^0_g and $R^0_{g'e}$ (eq 5). Such an offset is not observed in our TG data in Figure 5. This is probably due to the homodyne detection of the TG signal, that is, the signal is the modulus square of the response function convoluted with the electric fields. For example, a 15% constant contribution in the response function will only lead to a residual signal of 2%, which would be difficult to detect in a conventional TG measurement. To address this issue, PP measurements were carried out in ethanol at the same three wavelengths in the hope that the heterodyne nature of the signal would help to resolve this inconsistency.

IV. C. Wavelength-Dependent PP Measurements. As shown in Figure 8, the PP signals of 1144C in ethanol at all three wavelengths do not decay to zero within the population time range used, indicating a considerable contribution from the isomerized product state in the same spectral region. Furthermore, the offset at 580 nm is larger than that at 593 nm, indicating a larger product-state contribution at 580 nm. This supports the speculation in the above section that the abnormal peak shift in ethanol at 580 nm originates from a larger product-state contribution. The PP signal measured at 620 nm decays

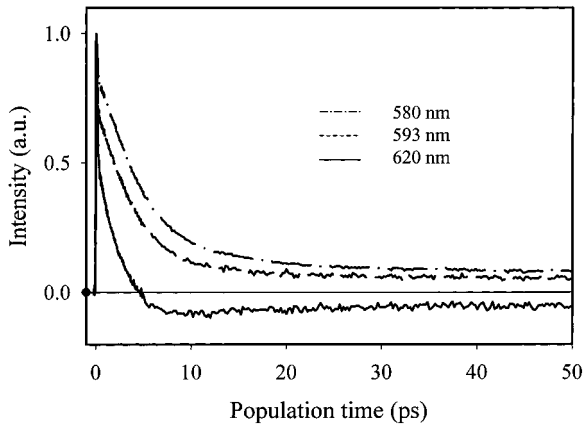

Figure 8. One-color pump−probe measurements for 1144C in ethanol at three wavelengths: 580, 593, and 620 nm.

TABLE 3: Pump−Probe Data for 1144C in Ethanol at Three Different Excitation Wavelengths [a]

wavelengths	A_1	τ_1(ps)	A_2	τ_2 (ps)	A_3	τ_3 (ps)
620 nm	160%	3.0	−55%	5.6	−5%	160
593 nm	89%	3.9	11%	170		
580 nm	91%	4.7	9%	76		

[a] Data were fitted to two or three exponential components.

to a negative value prior to relaxing back toward zero. An increased transient absorption when the detection wavelengths is tuned to the red edge of the absorption band can arise from hot ground-state absorption[39−41] during the recovery process or excited-state absorption.[30]

The PP data was fit using a sum of exponentials, and the fitting parameters are listed in Table 3. To avoid complications from the induction period in the recovery process,[18] the data was fitted after 800 fs. At all three wavelengths, we obtained a dominant component with a lifetime of ∼4 ps with a relative amplitude of ∼90%. A second component with lifetime ∼100 ps and a small amplitude was also resolved (the amplitude of this component is negative at 620 nm). We assign the first component to the ground-state recovery and the second to the back-reaction from the product state to the original ground state. Such an assignment is apparent from eq 4, where the sign of the last component could be either positive or negative depending on the relative amplitudes of $R^0_{g'e}$ and $R^0_{gg'e}$ at the specific wavelength. The product-state lifetime is not accurately determined, since the time window here is only 50 ps. In view of the likely high activation barrier from g' to g, the product-state lifetime may be much longer than 100 ps and could be significantly underestimated. An additional 5.6 ps component with negative amplitude was also required to fit the data at 620 nm. This component is attributed to the vibrational cooling process of the hot ground state.[39−41]

The GSR rates obtained from the PP data match quite well with the results obtained from the TG measurements. However, the PP signals seem to decay faster when the probe wavelength is located in the red part of the absorption spectrum, which as we discuss below is also due to contamination from the negative hot ground-state contribution.

V. Discussion

V. A. Rate-Determining Step of the GSR Process. The isomerization of 1144C in alcohol solvents has been extensively studied by Sundström et al. using different spectroscopic techniques, including fluorescence up-conversion,[29] stimulated emission,[27] pump−probe,[24,28] and excited-state absorption experiments.[28] The fluorescence and GSR lifetimes were found to be strongly solvent viscosity dependent, as predicted by the model proposed by Bagchi, Fleming, and Oxtoby (BFO).[18] This model describes a barrierless reaction associated with a large amplitude nuclear motion and has been useful in explaining many experimental observations. Its one-dimensional nature, however, precludes its quantitative application to wavelength-dependent data. The large amplitude bond-twisting motion makes the reaction rate inversely proportional to the viscosity of the solvent.[18] Sundström et al. concluded that the initial bond twisting (process 1) occurs on a subpicosecond time scale.[25,27,29] They suggest that the slowest step is the S_1–S_0 transition (process 2),[27,29] followed by relaxation on the ground state (process 3) that is even faster than that on the excited state because of the steeper potential-energy surface.[24,26,30]

This conclusion differs from the current view of the isomerization of *cis*-stilbene[42,43] and the triphenylmethane molecules,[22] also believed to be a barrierless large amplitude process. Here the rate-limiting step is believed to be the motion on the excited state to the region where a rapid nonadiabatic (or perhaps conical intersection) transition to ground-state surfaces occurs.[22,42] We believe a similar picture applies to 1144C with process 1 (the large amplitude torsional motion) being rate-limiting, rather than the internal conversion (process 2) for the following reasons. First, if the surface-transfer process is nonadiabatic, we expect it to obey the energy gap law.[44] In general, internal conversion rates in large molecules from S_n to S_1 are on the time scale of several hundred femtoseconds or less.[45−48] Even the rate of $S_1 \rightarrow S_0$ internal conversion in azulene is ∼1 ps with a large energy gap of ∼16000 cm^{-1}.[49,50] The internal conversion in 1144C (process 2) occurs where the energy gap between S_1 and S_0 is at a minimum. We expect the internal conversion rate to be at least similar to that between S_2 and S_1 states or even faster. Second, the internal conversion from S_1 to S_0 occurs without large geometry change and should not be very sensitive to the solvent viscosity. If process 2 is the rate-determining step, we expect the overall GSR time scale to be insensitive to the solvent viscosity, which is in contrast to the experimental observations. The strong dependence of GSR lifetime on solvent viscosity indicates that the rate-determining step is accompanied by a large amplitude motion, i.e. bond twisting. Furthermore, the strong temperature dependence of GSR lifetimes also argues against the possibility that internal conversion S_1–S_0 is the rate-determining step, since the internal conversion rate is not expected to be very sensitive to temperature. Third, since as depicted in Figure 1, the slope of the S_0 surface with respect to torsional angle is steeper than that of the S_1 surface, we expect the relaxation on the ground-state surface to be faster than that on the excited-state surface.[24,26,30] This is further supported by the observation that similar lifetimes were obtained from up-conversion, excited-state absorption, and ground-state recovery measurements.[27] Furthermore, given the fact that a considerable amount of product state also contributes to the signal, two different rates (process 3) will be associated with the recovery to the original ground state and the product state because of the different PES of the two ground states. The fact that only monoexponential decay associated with GSR is obtained in this work suggests that the dynamical processes occurring on the ground state are not likely to be the rate-determining step. Thus, we conclude that the slow decay on the excited-state surface (process 1) dominates the entire GSR process.

The two time constants resolved in TG measurements, ascribed to the time scales of SE and GSR, are strikingly different from each other (∼100 fs vs several picoseconds

depending on the solvent viscosity), although they both reflect dynamical processes occurring on the excited-state surface. The striking difference in the two time scales implies that the initially prepared population on the excited-state surface sweeps out of the laser spectral window quickly;[30] thus, only a small region on S_1 can be probed by SE in a one-color experiment. Furthermore, the SE lifetime is found to increase as the excitation wavelength is shifted to the blue, which is opposite to what is generally observed in nonreactive systems.[31,36] In nonreactive systems, a faster initial decay in the TG signal was usually observed for shorter excitation wavelengths. The initial decay in such systems was recently found to be influenced by the interference between the nonresonant solvent contribution and the wavelength-dependent resonant solute contribution.[31] Such different wavelength dependence of the time scales of SE and GSR suggests that the system is prepared on a different portion of the potential surface when the molecule is excited on the blue side of the absorption band. For example, high-frequency nonreactive modes may give access to a flatter region of the surface, slowing the initial decay rate. The insensitivity of the SE lifetime to temperature changes also suggests that this initial dynamics corresponds to the intramolecular vibrational relaxation or to a combination of vibrational relaxation with torsional motion, aspects of the system which are not included in the one-dimensional BFO model.[51]

V. B. Product-State Contribution. We now return to the unusual 3PEPS response at 580 nm. Recall that the peak shifts in ethanol are higher than those in hexanol at 580 nm at most population times, while the peak shift data at 593 and 620 nm are very similar for the two solvents. The higher peak shifts in ethanol could be caused by a higher rephasing capability or a larger negative free induction decay (FID) contribution. It is unlikely that the rephasing capabilities are similar at 593 and 620 nm and suddenly become different at 580 nm for the two solvents. We propose instead that the higher peak shift arises from a larger negative FID contribution.

The rephasing and FID terms will interfere in the total response function. The maximum signal for the rephasing term is located at a finite positive coherence time and gives a finite value for the peak shift, while the FID term decays monotonically and peaks at zero coherence time.[5] The sum of a rephasing term and a positive FID term makes the total signal peak at a shorter coherence time and thus gives a smaller value of the peak shift. In contrast, the sum of a rephasing term and a negative FID term will result in a larger value of the peak shift.[7]

The question remaining is the origin of this negative FID contribution. In a previous paper,[7] we demonstrated that excited-state absorption could contribute a negative FID term. Excited-state absorption of 1144C has been observed on the blue side of the absorption spectrum[27−29] and is very likely to contribute to the signal measured at 580 nm. However, the absence of the characteristic rise behavior of excited-state absorption in the TG signal[7] at 580 nm suggests excited-state absorption is not the only contribution responsible for such a difference. The PP results in ethanol suggest a larger product-state absorption at 580 nm than at 593 nm. Photoisomer absorption can contribute to the response function in a similar way as the excited-state absorption does. As discussed in the theoretical section, the decay of the excited state to the isomer ground state leads to a negative contribution $-R_{g'e}$ because of the odd number of interactions on the ket and bra sides of the double-sided Feynman diagram. Since g−e and g′−e′ absorption are associated with different electronic transitions, they are not expected to be fully correlated with each other, and $R_{g'e}$ should contribute as an FID signal. A pronounced negative FID contribution results in a higher peak shift, and the larger peak shifts obtained in ethanol compared to hexanol indicates more negative FID contribution from $R_{g'e}$, that is, a higher product yield in ethanol. However, the striking difference in the 3PEPS data starting from ∼50 fs (Figure 7) strongly suggests the excited-state absorption also contributes significantly at short times. The characteristic rise behavior[7] is probably masked by the subsequent photoisomer absorption. The different excited-state absorption contribution in two solvents suggests that the potential-energy surface is significantly solvent-dependent.[43]

These arguments imply that the branching ratio between the isomer and normal ground states of 1144C in ethanol and hexanol is quite similar when the excitation wavelength is 593 or 620 nm, while a higher branching ratio was obtained in ethanol at 580 nm. The fact that the 3PEPS result obtained in hexanol does not look unusual at 580 nm suggests that only a small change in the branching ratio occurs in this solvent which is not enough to change the decay behavior of the peak shift.

A larger negative FID could also result from dramatically different absorption coefficients of the isomer product state in the two solvents at 580 nm. This possibility does not seem very likely considering the similar structures of the reactant and isomerized product. Instead, it seems reasonable to assume that the absorption spectrum of the product is slightly shifted from that of the reactant. Most importantly, a larger absorption coefficient for the isomer product state implies a larger $R^0_{g'e}$ contribution and gives a smaller residual signal ($R^0_g - R^0_{g'e}$, see eq 5) in the pump−probe data at 580 nm compared to those at 593 and 620 nm, which is opposite to the experimental results (Figure 8). The combination of the 3PEPS and PP data supports the proposal that the abnormal 3PEPS data at 580 nm arises from a larger branching ratio at this wavelength.

Both wavelength and solvent (viscosity) dependent results suggest a multidimensional nature to the potential-energy surface[51] in this system. For example, in low viscosity solvents, excitation at 580 nm may cause the molecule to approach the surface-crossing region with a different trajectory from that for the longer wavelength excitation. Higher product yield with shorter excitation wavelength was also observed in the isomerization of benzene, which has been used as the evidence of existence of a conical intersection participating in the radiationless deactivation process.[52,53] Our knowledge of the potential-energy surfaces of 1144C is far too rudimentary to discuss this point further.

V. C. Transient Grating (TG) and Pump−Probe (PP) Signals. The TG and PP results show apparently different wavelength dependence for 1144C. The decay of the PP signal becomes faster as the excitation wavelength is shifted to the red, and the signals become negative at longer population times at 620 nm. In contrast, the TG signal is less sensitive to the excitation wavelength, and the decay in the picosecond time region becomes slightly slower at longer wavelengths. The homodyne TG signal cannot be simply understood as the square of the PP signal, especially when excited at the red edge of the spectrum. For example, at 620 nm, the negative contribution in the PP signal does not cause the TG to decay to zero and then rise again in the corresponding population time region.

By separately tuning the excitation and detection wavelengths, the GSR rate has been observed to be insensitive to the excitation wavelength,[22,54] while it becomes apparently faster as the detection wavelength is tuned to the red.[22,24] This was explained as being due to GSR mixing with stimulated emission on the red side of the absorption spectrum.[22,24] Our data cannot

exclude the possibility that the SE contains a dominant fast component and a small slow component; however, SE contamination itself cannot explain the observation that the PP signal at longer wavelengths decays to a negative value and recovers back toward zero. It is more reasonable to ascribe the contamination as arising from the negative hot ground-state contribution as the wavelength shifts to the red, since the relaxation on the ground state will unavoidably pass a region where the transition is resonant with the red part of the absorption spectrum. The cooling process should also exist when excitation is on the blue side of the spectrum but will contribute as a small positive component, as reported earlier in measurements on malachite green.[55] This component is not well resolved for excitation at 580 and 593 nm in the current system probably because the cooling rate (~5.6 ps) is just slightly slower than the GSR rate (~4 ps). The GSR process in the PP signal appears faster at longer wavelengths mainly because of the contamination from the hot ground-state absorption and its relaxation to the equilibrium spectrum. In addition, the possibility of a small contamination from SE cannot be excluded.

The observed faster decay with blue excitation wavelength in the TG signal does not necessarily indicate an increase of the recovery rate. Instead, it is probably due to a change in the contribution of the real component of $P^{(3)}$,[35] which does not contribute to the PP signal. When the excitation wavelength is detuned from the absorption maximum, the population grating will contribute to both the real and imaginary parts of the third-order polarization $P^{(3)}$. The real and imaginary components are related to each other by the Kramers−Kronig relation.[3,56] The sign of the real part is excitation wavelength-dependent, being negative on the red side of the absorption band and positive on the blue edge, as observed in the frequency-resolved heterodyne TG by Vauthey et al.[57] and in our recent wavelength-dependent heterodyne TG measurements.[35] This wavelength dependence of the real component produces different decay behavior in the real and imaginary components of the total third-order polarization $P^{(3)}$ in a multilevel system. In a system where a rapid radiationless transition brings the molecules from the excited state to the original ground state, the transient hot ground-state absorption will also contribute to the signal, with a spectrum red-shifted with respect to the relaxed spectrum. In the current system, 1144C, 620 nm is located on the red side of the relaxed ground-state absorption spectrum, but lies on the blue side of the transient hot ground-state spectrum. The Kramers−Kronig relation implies that the real part associated with the relaxed transition is negative at 620 nm but positive at this wavelength for the hot ground-state contribution. This positive transient dispersion contribution will give a rise in the negative signal of the real component, analogous to the way a transient excited-state absorption gives a rise in the decay of the PP signal. This rise behavior in the real component of the heterodyne TG signal for excitation at the red edge of the absorption spectrum has been observed in our study of the relaxation of the triphenylmethane (TPM) molecules.[35] The hot ground-state absorption contributes in opposite ways to the real and imaginary component of TG signal, that is, a rise in the real part and negative going signal in the imaginary part, thus producing an opposite wavelength dependence in the TG and PP signals.

In 1144C, a portion of the excited molecules will also relax to the ground state of the photoisomer first, before eventually relaxing back to the original ground state on a slower time scale. The relaxation along this pathway will also pass through a region that will give a hot ground-state absorption. The hot ground-state absorption on the photoisomer side will contribute to the total signal in a similar way to that from molecules relaxing to the original ground state. In addition, the absorption spectrum of the relaxed isomer was observed to be slightly red-shifted with respect to that of the original ground state,[28,29] and the product state will also contribute to the faster decay in the PP data at 620 nm and to the difference between the PP and TG signals, in a similar way to the hot ground state.

Therefore, we conclude that the apparently contradictory wavelength-dependent GSR rate obtained from the TG and PP data results from the contributions of the hot ground state and the product state. The faster decay observed in the PP data at 620 nm for the first 5 ps is mainly due to the decay into the hot ground state and the product state. Equilibration of the hot ground state is expected to be complete within 10 ps, while the recovery of the product state to the original ground state takes place on a much longer time scale. This gives rise to the wavelength-dependent residual signal at longer times (50 ps) in the PP data (negative at 620 nm and positive at 580 and 593 nm). The real GSR rate is probably relatively insensitive to both the pump and probe wavelength, as suggested by earlier work.[58,59]

A final feature of our data is the oscillatory behavior in the TG and 3PEPS signals which has a frequency of 220 cm^{-1} and persists up to ~1 ps. The oscillations are seen in both solvents at all three excitation wavelengths. The modulation is more pronounced when the excitation wavelength is on the red side of the absorption band.

VI. Conclusions

It has been demonstrated by Joo et al.[5] that three-pulse photon echo peak shift, transient grating, and pump−probe techniques measure the same solvation dynamics information in a simple two-level system. In this work, we carried out a 3PEPS, TG, and PP study on the isomerization reaction of 1144C. A double-sided Feynman diagram analysis was used to formulate the response functions for the contributions from various regions of the potential surfaces to the third-order signal. A simple kinetic model was used to connect the different regions of the potential surfaces. Very different and apparently contradictory wavelength dependencies were obtained in the decay profiles from the different techniques. We found that the dynamics on this simple system are quite complicated and that it is easy to arrive at misleading conclusions based on the results from any single technique. The combination of the three different techniques provides complimentary information and allows a consistent picture to be developed.

Specifically, the ambiguous contributions of the recovery to the original ground state or to the spectrally overlapped product state in TG measurements can be distinguished in our 3PEPS experiments because of the different rephasing capability associated with these two contributions. The combination of these types of measurements leads to the conclusion that a larger product yield is obtained when the excitation wavelength is shifted to the blue or when the solvent viscosity is decreased.

The analysis of the solvent and temperature dependence of the GSR rates showed that a monoexponential decay is adequate to describe the recovery process. The ground-state recovery is solvent viscosity and temperature dependent. The bond-twisting process on the excited-state surface is the rate-limiting step of the entire recovery process, rather than the internal conversion process as previously proposed.[27,29]

The wavelength dependence of the decay shows opposite trends in TG and PP for the current system. When the excitation wavelength is shifted to the blue, the PP signal decays more

slowly and the TG signal decays more rapidly. The hot ground-state absorption and its cooling process, as well as the product-state contribution, are found to contribute in opposite ways to the real and imaginary components of third-order polarization $P^{(3)}$, with respect to the contributions from the stimulated emission and ground-state bleaching, when excited at the red part of the absorption spectrum. This difference is responsible for the different decay behavior found in the two measurements. A similar difference in the TG and PP signals was also observed in malachite green and crystal violet and may be typical of systems with rapid decays to the ground state. A further study of these systems using heterodyne TG to separately measure the real and imaginary parts has been carried out on the triphenylmethane molecules and will be presented elsewhere in detail.[35]

Acknowledgment. This work was supported by a grant from NSF. We thank Professor Gregory D. Scholes and Dr. Mino Yang for many helpful discussions and Dr. Ying-Zhong Ma and Dr. Kaoru Ohta for a critical reading of the manuscript.

References and Notes

(1) Rullière, C. *Femtosecond laser pulses: principles and experiments*; Springer: Berlin, New York, 1998.
(2) Fleming, G. R. *Chemical applications of ultrafast spectroscopy*; Oxford University Press: New York, 1986.
(3) Mukamel, S. *Principles of nonlinear optical spectroscopy*; Oxford University Press: New York, 1995.
(4) Eichler, H. J.; Günter, P.; Pohl, D. W. *Laser-induced dynamic gratings*; Springer-Verlag: Berlin, New York, 1986.
(5) Joo, T. H.; Jia, Y. W.; Yu, J. Y.; Lang, M. J.; Fleming, G. R. *J. Chem. Phys.* **1996**, *104*, 6089.
(6) Myers, A. B.; Hochstrasser, R. M. *IEEE J. Quantum Electron.* **1986**, *QE−22*, 1482.
(7) Xu, Q. H.; Scholes, G. D.; Yang, M.; Fleming, G. R. *J. Phys. Chem. A* **1999**, *103*, 10348.
(8) Cho, M. H.; Yu, J. Y.; Joo, T. H.; Nagasawa, Y.; Passino, S. A.; Fleming, G. R. *J. Phys. Chem.* **1996**, *100*, 11944.
(9) Fleming, G. R.; Passino, S. A.; Nagasawa, Y. *Philos. Trans. R. Soc. London, Ser. A* **1998**, *356*, 389.
(10) Yang, M.; Fleming, G. R. *J. Chem. Phys.* **1999**, *111*, 27.
(11) de Boeij, W. P.; Pshenichnikov, M. S.; Wiersma, D. A. *Chem. Phys. Lett.* **1996**, *253*, 53.
(12) de Boeij, W. P.; Pshenichnikov, M. S.; Wiersma, D. A. *J. Phys. Chem.* **1996**, *100*, 11806.
(13) Yang, M.; Ohta, K.; Fleming, G. R. *J. Chem. Phys.* **1999**, *110*, 10243.
(14) Xu, Q.-H.; Fleming, G. R. unpublished results.
(15) Wang, Q.; Schoenlein, R. W.; Peteanu, L. A.; Mathies, R. A.; Shank, C. V. *Science* **1994**, *266*, 422.
(16) Haran, G.; Morlino, E. A.; Matthes, J.; Callender, R. H.; Hochstrasser, R. M. *J. Phys. Chem. A* **1999**, *103*, 2202.
(17) Kochendoerfer, G. G.; Mathies, R. A. *Isr. J. Chem.* **1995**, *35*, 211.
(18) Bagchi, B.; Fleming, G. R.; Oxtoby, D. W. *J. Chem. Phys.* **1983**, *78*, 7375.
(19) Todd, D. C.; Fleming, G. R. *J. Chem. Phys.* **1993**, *98*, 269.
(20) Waldeck, D. H. *Chem. Rev.* **1991**, *91*, 415.
(21) Pollak, E. *J. Chem. Phys.* **1987**, *86*, 3944.
(22) Ben-Amotz, D.; Harris, C. B. *J. Chem. Phys.* **1987**, *86*, 4856.
(23) Duxbury, D. F. *Chem. Rev.* **1993**, *93*, 381.
(24) Åberg, U.; Sundström, V. *Chem. Phys. Lett.* **1991**, *185*, 461.
(25) Åberg, U.; Åkesson, E.; Alvarez, J. L.; Fedchenia, I.; Sundström, V. *Chem. Phys.* **1994**, *183*, 269.
(26) Åberg, U.; Åkesson, E.; Fedchenia, I.; Sundström, V. *Isr. J. Chem.* **1993**, *33*, 167.
(27) Åberg, U.; Åkesson, E.; Sundström, V. *Chem. Phys. Lett.* **1993**, *215*, 388.
(28) Alvarez, J. L.; Yartsev, A.; Åberg, U.; Åkesson, E.; Sundström, V. *J. Phys. Chem. B* **1998**, *102*, 7651.
(29) Yartsev, A.; Alvarez, J. L.; Åberg, U.; Sundström, V. *Chem. Phys. Lett.* **1995**, *243*, 281.
(30) Ben-Amotz, D.; Harris, C. B. *Chem. Phys. Lett.* **1985**, *119*, 305.
(31) Xu, Q.-H.; Ma, Y.-Z.; Fleming, G. R. *J. Chem. Phys.* **2001**, submitted.
(32) Joo, T. H.; Jia, Y. W.; Yu, J. Y.; Jonas, D. M.; Fleming, G. R. *J. Phys. Chem.* **1996**, *100*, 2399.
(33) Agarwal, R.; Yang, M.; Xu, Q. H.; Fleming, G. R. *J. Phys. Chem. B* **2001**, *105*, 1887.
(34) Yang, M.; Fleming, G. R. *J. Chem. Phys.* **2000**, *113*, 2823.
(35) Xu, Q.-H.; Ma, Y.-Z.; Fleming, G. R. **2001**, in preparation.
(36) Larsen, D.; Ohta, K.; Xu, Q.-H.; Fleming, G. R. *J. Chem. Phys.* **2001**, *114*, 8008.
(37) Xu, Q.-H.; Fleming, G. R. unpublished results.
(38) Ohta, K.; Larsen, D.; Yang, M.; Fleming, G. R. *J. Chem. Phys.* **2001**, *114*, 8020.
(39) Walker, G. C.; Åkesson, E.; Johnson, A. E.; Levinger, N. E.; Barbara, P. F. *J. Phys. Chem.* **1992**, *96*, 3728.
(40) Reid, P. J.; Silva, C.; Barbara, P. F.; Karki, L.; Hupp, J. T. *J. Phys. Chem.* **1995**, *99*, 2609.
(41) Kovalenko, S. A.; Schanz, R.; Farztdinov, V. M.; Hennig, H.; Ernsting, N. P. *Chem. Phys. Lett.* **2000**, *323*, 312.
(42) Raftery, D.; Sension, R. J.; Hochstrasser, R. M. Chemical Aspects of Solution Phase Reaction Dynamics. In *Activated barrier crossing: applications in physics, chemistry, and biology*; Fleming, G. R., Hanggi, P., Eds.; World Scientific: River Edge, NJ, 1993; p 163.
(43) Saltiel, J.; Waller, A. S.; Sears, D. F., Jr. *J. Am. Chem. Soc.* **1993**, *115*, 2453.
(44) Freed, K. F. In *Radiationless processes in molecules and condensed phases*; Fong, F. K., Ed.; Springer: Berlin, 1976; p 23.
(45) Shank, C. V.; Ippen, E. P.; Teschke, O. *Chem. Phys. Lett.* **1977**, *45*, 291.
(46) Laermer, F.; Elsaesser, T.; Kaiser, W. *Chem. Phys. Lett.* **1989**, *156*, 381.
(47) Laermer, F.; Israel, W.; Elsaesser, T. *J. Opt. Soc. Am. B, Opt. Phys. (USA)* **1990**, *7*, 1604.
(48) Kang, T. J.; Ohta, K.; Tominaga, K.; Yoshihara, K. *Chem. Phys. Lett.* **1998**, *287*, 29.
(49) Wurzer, A. J.; Wilhelm, T.; Piel, J.; Riedle, E. *Chem. Phys. Lett.* **1999**, *299*, 296.
(50) Schwarzer, D.; Troe, J.; Schroeder, J. *Ber. Bunsen-Ges.* **1991**, *95*, 933.
(51) Bagchi, B.; Fleming, G. R. *J. Phys. Chem.* **1990**, *94*, 9.
(52) Smith, B. R.; Bearpark, M. J.; Robb, M. A.; Bernardi, F.; Olivucci, M. *Chem. Phys. Lett.* **1995**, *242*, 27.
(53) Bernardi, F.; Olivucci, M.; Robb, M. A. *Chem. Soc. Rev.* **1996**, *25*, 321.
(54) Sundström, V.; Gillbro, T. *J. Chem. Phys.* **1984**, *81*, 3463.
(55) Xu, Q.-H.; Ma, Y.-Z.; Fleming, G. R. *Chem. Phys. Lett.* **2001**, *338*, 254.
(56) Loudon, R. *The quantum theory of light*, 2nd ed.; Clarendon Press: Oxford, U.K., 1983.
(57) Högemann, C.; Pauchard, M.; Vauthey, E. *Rev. Sci. Instrum. (U.S.)* **1996**, *67*, 3449.
(58) Sundström, V.; Gillbro, T.; Bergström, H. *Chem. Phys.* **1982**, *73*, 439.
(59) Doust, T. *Chem. Phys. Lett.* **1983**, *96*, 522.